Northumbria Research Link

Evaluating the Effect of Electric Vehicle Parking Lots in Transmission-Constrained AC Unit Commitment under a Hybrid IGDT-Stochastic Approach

Masoumeh Ahrabi[a], Mehrdad Abedi[a], Hamed Nafisi[a], Mohammad Amin Mirzaei[b], Behnam Mohammadi-Ivatloo[b,c], Mousa Marzband[d,e]

[a]*Department of Electrical Engineering, Amirkabir University of Technology, Tehran, Iran*
[b]*Faculty of Electrical and Computer Engineering, University of Tabriz, Tabriz, Iran*
[c]*Institute of Research and Development, Duy Tan University, Da Nang, 550000, Vietnam*
[d]*Northumbria University, Electrical Power and Control Systems Research Group, Ellison Place NE1 8ST, Newcastle upon Tyne, United Kingdom*
[e]*Center of research excellence in renewable energy and power systems, King Abdulaziz University, Jeddah, Saudi Arabia*

Abstract

Power network operators have recently faced new challenges due to an increase in the penetration of non-dispatchable renewable energy sources in power grids. Incorporating emerging flexible resources like electric vehicle parking lots (EVPLs) and demand response programs (DRPs) into power systems, could be a good solution to deal with inherent uncertainties imposed by these resources to the power grid. EVPLs can improve power system operating conditions by active and reactive power injection capabilities. The participation of consumers in DRPs can also improve energy consumption management by decreasing or shifting loads to other periods. This paper proposes a hybrid information gap decision theory (IGDT)-stochastic method to solve a transmission-constrained AC unit commitment model integrated with electric vehicle (EV), incentive-based DRP, and wind energy. The behavioural uncertainty related to EV owners is modelled using a scenario-based method. Additionally, an IGDT method is applied to manage wind energy uncertainty under a two-level optimization model. Verification of the proposed model is done under several case studies. Based on the results achieved, the proposed risk-based hybrid model allows the operator to differentiate between the risk level

Email address: `mousa.marzband@gmail.com Corresponding author` (Mousa Marzband)

of existing uncertainties and apply a high-flexibility decision-making model to deal with such difficulties. Additionally, the role of the aforementioned flexible resources in the reduction of power system running costs and wind power uncertainty handling are evaluated. Numerical results confirm a 3.7% reduction in the daily operating costs as a consequence of coordinated scheduling of EVPL and DRP. Moreover, Taking advantage of reactive power injection of EVPL provides more cost savings.
Keywords: Information-gap decision theory, electric vehicle parking lot, demand response program, renewable energy resource, stochastic programming, emerging flexible resources.

Nomenclature

Index

b, b’	Bus index
n	Electric vehicle index
p	Index for modeling of loads minimum on time and off time
u	Index for modeling of thermal units minimum on time and off time
j	Load index
pl	Parking lot index
l	Power line index
g	Power unit index
s	Scenario index
NEV	Set of electric vehicles
NL	Set of lines
NJ	Set of loads
NPL	Set of parking lots
NS	Set of scenarios
NU	Set of power units
NT	Set of time intervals
NW	Set of wind power plants

Parameters

t	Time index
w	Wind power plant index
$Cap^{EV}_{n,t_n^{arv},t_n^{dep},s}$	Battery capacity of EV that enter PL at t^{arv} and exit at t^{dep} (KWh)
$\lambda_{j,t}$	Cost of load participation in DR ($/MWh)
$t_n^{arv/dep,min}$, $t_n^{arv/dep,max}$	Determined range for the entry/exit time of EVs (h)
$SOC_n^{arv/dep,min}$, $SOC_n^{arv/dep,max}$	Determined range for the initial/final SOC of EVs (%)
$\lambda^{dis}_{pl,t}$	Discharging cost of parking lot ($/MWh)
$\eta^{dis/ch}$	Discharging/charging efficiency of EVs
$\xi^{dis/ch}$	Discharging/charging rate of EVs (KW/h)
γ	DR participation factor (%)
$t_{pl}^{arv/dep}$	Entry/exit time of EVs (h)
$D_{j,t}$	Expected hourly load (MW)
$\widehat{P}_{w,t}$, $\widehat{Q}_{w,t}$	Forecasted active/reactive power of wind generation (MW, KVar)
Z_l	Impedance of lines (Ω)
φ_j	Load angle (deg)
S_l^{max}	Maximum capacity of lines (MVA)
N_{pl}^{max}	Maximum car capacity of PL
S_{pl}^{max}	Maximum tradable apparent power between PL and grid (MVA)
$\mu_{arv/dep/SOC_{arv/dep}}$	Mean value of the EV owners uncertain parameters
$R_g^{up/dn}$	Minimum ramp up/down of power units (MW/h)
MUT_j, MDT_j	Minimum on/ off time of shiftable load (h)
MUT_g, MDT_g	Minimum up/ down time of power units (h)
$DR_j^{min\,/\,max}$	Minimum/ Maximum curtailed load (MW)
OF_b	Objective function in the base condition ($)
SU_g, SD_g	On/ Off cost of power units ($)
$\overline{\Psi}$	Predicted amount of the uncertain parameter Ψ
π_s	Probability of scenarios
$\Delta d_j^{up/dn}$	Ramp limits of load (MW)
$d_{r/\rho}$	Robustness/ opportuneness parameter in RA//RS strategy

$\Delta^{r/\rho}$	Satisfactory value of the objective function in RA/RS strategy
U	Set of input uncertain parameter
$SOC^{EV}_{n,t_n^{arv},t_n^{dep},s}$	SOC of EV that enter PL at t^{arv} and exit at t^{dep} (%)
$SOC_n^{arv/dep}$	Initial/final SOC of EVs (%)
c_g, b_g, a_g	Thermal units operation cost coefficients ($, $/MWh and $/(MWh)^2)
$Cap_{pl,t,s}$	Total battery capacity of PL (MWh)
$N_{pl,t,s}$	Total number of EVs in the PL
$N^{arv/dep}_{pl,t,s}$	Total number of EVs arrive/departure to/from PL at a distinct time
$N^{EV}_{t_n^{arv},t_n^{dep},s}$	Total number of EV that enter PL at t^{arv} and exit at t^{dep}
P_g^{max}, P_g^{min}	Upper/ lower bound for active power of thermal units (MW)
Q_g^{max}, Q_g^{min}	Upper/lower bound for reactive power of thermal units (MVar)
$SOC_{pl}^{min/max}$	Upper/ lower bound for SOC of EVPL (%)
V_b^{max}, V_b^{min}	Upper/ lower bound for voltage magnitude of buses (pu)
δ_b^{max}, δ_b^{min}	Upper/ lower bound for voltage angle of buses (deg)
$\sigma^2_{arv/dep/SOC_{arv/dep}}$	Variance of the EV owners uncertain parameters
Decision variables	
$D^r_{j,t,s}$, $Q^r_{j,t,s}$	Active/ reactive load after DR implementation (MW/MVar)
$PF_{l,t,s}$, $QF_{l,t,s}$	Active/ reactive power flow at line l (MW/MVar)
$P_{w,t}$	Actual active power of wind generation (MW)
$Z_{g,t}$	Binary variable that represents on/ off status of thermal units
$Z^{on}_{j,t,s}$, $Z^{off}_{j,t,s}$	Binary variable that describes on/ off time of load
$U^{PL2G/G2PL}_{pl,t,s}$	Binary variable that shows PL2G/ G2PL mode of EVPL
$Y_{j,t}$	Binary variable that describes status of loads participation in DR
F_g^c	Cost function of power units ($)
$P^{PL2G/G2PL}_{pl,t,s}$	EVPL active power in PL2G/ G2PL mode (MW)
$Q^{PL2G/G2PL}_{pl,t,s}$	EVPL reactive power in PL2G/G2PL mode (KVar)
β, α	Optimum opportuneness/ robustness function
$P_{g,t,s}$, $Q_{g,t,s}$	Scheduled active/ reactive power of thermal units (MW/MVar)
$DR_{j,t,s}$	Shiftable load (MW)
$SUC_{g,t}$, $SDC_{g,t}$	Start-up/ shut-down cost of thermal generation unit ($)
$SOE_{pl,t,s}$	State of energy of EVPL (MWh)

ε	Unknown radius of the uncertain parameter
$\delta_{b,t,s}$, $V_{b,t,s}$	Voltage angle/ magnitude of buses (deg/pu)

1. Introduction

1.1. Overview

In recent decades, the global warming problem resulted from excess greenhouse gas emissions has become one of the most critical challenges. The United States environmental protection agency published a report in 2018, which shows that transportation services and electricity generation sectors were two main greenhouse gas sources, releasing almost 55% of the total emissions in that year [1]. Hence replacing fossil fuels by renewable energy sources (RESs) and electrification of transportation can deal with the greenhouse gas issues well [2–4]. The increasing universal trend in RESs utilization has imposed various challenges on the power system because of the variable nature of these resources [5]. There are some measures to address this issue such as raising the flexibility of the energy suppliers under the lowest operating cost [6], applying modified models in the process of unit commitment (UC) [7] and modeling the uncertainty related to the system and integrating emerging flexible resources like electric vehicle parking lots (EVPLs) and demand response programs (DRPs) into power system operation [8]. Coordinated scheduling of these resources covers the challenges related to the RESs.

EVs can supply active and reactive power for the grid and improve power system operating conditions consequently and because of the small capacity of each electric vehicle (EV), extensive use of EVs as a parking lot (PL) will have more challenges and opportunities for the power system [9, 10]. EVPLs as an aggregator that collects EVs to reach high storage capacity can act as a controllable load with the potential of fast responding to the power injection need. Moreover, most EVs are available in parking lot areas for more than 95% of the time during a day [11]. These advantages can provide precious opportunities for the power system. In addition, consumers can shift their electricity use from the on-peak period or renewable generation deficiency hours to off-peak period or surplus renewable generation hours and decrease renewable generation spillage and energy cost of the system by participating in the DRP [12, 13]. To this end, in this paper, the effect of flexible technologies such as EVPLs and DRPs under a coordinated approach in an AC transmission constrained unit commitment (AC-TCUC) problem is analyzed. The wind power uncertainty is modeled as an information gap decision theory (IGDT)-based technique, and the uncertain behavior of EV owners is modeled through a scenario-based approach.

1.2. Literature review

There are various researches on the assessment of smart technologies' impacts on the power grid operation in the last decades. A stochastic UC problem accompanied by an EVPL and renewable energy generation is presented in [14], where the uncertainties of the RESs and EV owners are considered through a scenario-based method. Authors in [15] presented a two-level method for EVPL in distribution systems considering parking lot (PL) participation in energy, reserve, and regulation distribution markets. In the first level, EVs characteristics are modeled, and in the second level, a new approach is implemented to address the constraints of the distribution systems while minimizing the total cost. A day-ahead EV charging scheduling using a game model is proposed in [16], which evaluates the impact of EVs on electricity prices. Authors of [17] focused on the charging scheduling of EVs with the purpose of supplying frequency regulation services. A new two-level approach for the operation of a distribution company integrated with EVPL and RES is presented in [18] in which the power purchasing cost is minimized in the upper-level, and parking lot (PL) owner profit is maximized in the lower-level. The investigation of an optimal strategy of an EV aggregator in the electricity market considering price uncertainty is performed in [19] under a scenario-based stochastic method, and the risk of uncertainties is considered by downside risk constraints implementation. Authors in [20] proposed a new approach to integrate EVs in the day-ahead scheduling of the wind-based power. This literature considered market price and wind power uncertainty under a stochastic optimization model. A robust optimization approach is developed in [21] to evaluate the robust scheduling of EV aggregators with consideration of uncertainties related to price. The uncertainty problem of EV aggregators is solved in [22] by implementing the interval optimization approach, and robust scheduling of EV aggregator is achieved. Authors in [23] proposed a new framework for optimal scheduling of EVs and RES in the distribution system, and its goal is to minimize the operating cost of the system. A model for calculating the optimized scheduling of EVs' active power along with reactive power supply function is provided by [24], and the main goal is minimizing owners' cost. The impact of EVs on the power loss reduction of a microgrid is evaluated in [25] under a two-stage optimization approach. EVs reactive power allocation is considered in this literature.

The effect of DRP on a UC problem with the aim of maximizing social welfare is investigated in [26] under a two-level approach. A stochastic market-clearing model using the scenario generation approach considering EVPL, DRP, and energy storage systems (ESS) is provided by [9], where a DC-power flow is applied to model the constraints of the network. A stochastic security-constrained DC-UC problem integrated with RES, DRP, and hydrogen ESS is solved in [27]. In this literature, DC constraints are considered for power flow calculation. A techno-economic model for the optimal scheduling of a distribution company is proposed in [28] in the presence of RESs and EVPLs with considering uncertainties of them. Authors in [29] presented two decentralized algorithms for the utilization of EVPLs as a distributed energy supplier in the presence of DRP in which EV owners' uncertainty is modeled through a modified latent semantic analysis. A price-based DR model to optimize the charging strategy of EVs is proposed in [30], where a statistical approach is considered for modeling the charging behavior of EV owners. The DRPs and EVPLs impact on minimizing system operating cost and emission is evaluated in [31] under a DC-UC problem. Scheduling of the electricity market in the presence of RESs and DRP is done in [32] under a two-stage stochastic model. In [33], stochastic scheduling of power systems considering DRP and ESS is provided for handling the uncertainty of RES. An adaptive robust optimization technique for the UC problem is developed in [34], incorporating wind power uncertainty. A new method to model renewable generation uncertainty in day-ahead robust UC is developed in [35]. A robust AC-UC model for managing the uncertainty of wind output is presented in [36], where EVPL and DRP are ignored.

In almost all of the above literature, well-known robust optimization and stochastic approaches are applied for modeling the uncertainties of the power system. IGDT is a non-probabilistic method that can be implemented to model uncertainties of the power system. There is no requirement for probability density function (PDF) or scenario generation in this approach. That is why the computational time in the IGDT method is much lower than conventional approaches. Moreover in IGDT, the radius of uncertain parameters should not be predefined. In other words, in this method, the maximum uncertainty radius of the uncertain parameters will be determined by satisfying the objective function in the predefined interval. This can be useful for the independent system operator (ISO) in the decision-making process. This approach is a sufficient method to deal with various problems in power system operation and utilization such as market participants bidding strategies [37], UC problems [38], RESs dispatch in power system, and microgrids [39], and integrated power and gas systems [40]. A new framework for multi-objective UC is proposed in [41], considering wind generation and EVs. Uncertainties of wind output and load demand are considered utilizing IGDT. A security-constrained UC problem considering wind farm is solved in [42], where the uncertainty of wind power generation is modeled through IGDT approach. Finally, in [43], the IGDT method is implemented for scheduling of thermal generation units, DR decisions, and grid parameters.

1.3. Contribution

There are a number of gaps in the reviewed literature; however, some of the main gaps are expressed below:

- ✓ Some of the reviewed literature e.g. [3, 8, 9, 11, 12, 14–21, 28–30, 40, 42] has evaluated the impact of aggregated EVs on power system utilization ignoring the capability of reactive power injection for EVs, while EVs can provide reactive power support without battery wear.

- ✓ Although a few works of literature e.g. [8, 28–30, 42], has focused on coordinated scheduling of EVPL and DRP and its impact on network operation condition, this evaluation has been done under a DC-UC framework, while the assumption needed for DC load flow analysis takes the model away from reality.
- ✓ Most of the reviewed literature, e.g. [18, 20, 30–32, 35–38] has only applied one of well-known traditional approach or IGDT under a robust attitude for modeling power system uncertainties, while ISO is reluctant to implement an identical conservatism level to manage system uncertainties, and also power grid uncertainties are not against the ISO benefit in all situations.

To cover these challenges, this paper presents the simultaneous operation of EVPL and incentive-based demand response program (IDRP) in a transmission-constrained unit-commitment model under an AC optimal power flow (OPF) approach that is shown in Figure 1. Uncertainties of wind power generation and EV owners' behavior are considered in this study. Table 1 compares the main contributions of the proposed model and the literature by taking in mind the remarkable contribution of models. The main contributions of this paper are clearly provided below:

- ✓ Developing a framework for reactive power injection via EVPL, by considering technical limits, and EV owners' desirables, and evaluating its impact on power system operation conditions and system operation cost reduction.
- ✓ Applying IDRP for active and reactive loads in AC-TCUC that eliminates wind power uncertainty effect and decreases operation cost. This makes the proposed model more realistic since most of the power system loads have a power factor of less than unit.
- ✓ Taking advantage of both IGDT and stochastic programming approaches under a two-level hybrid IGDT-stochastic optimization problem. This provides high-flexibility decision-making for ISO and facilitates differentiation between the risk level of existing uncertainties.
- ✓ Considering uncertainties of both wind power and EV owners' behavior so that wind power uncertainty is modeled through an IGDT-based method un-

der both risk-averse (RA) and risk-seeker (RS) strategies, and uncertain behavior of EV owners are addressed by scenario-based approach.

Table 1: Comparison of the previous reports with the current work

References	UC problem	Power flow		EVPL	DRP	Uncertainty			Uncertainty modeling
		DC	AC			Wind	EV owners	Load	
[9]	✓	✓	×	✓	✓	×	✓	×	Two-stage stochastic
[32]	✓	✓	×	×	✓	✓	×	×	Two-stage stochastic
[34]	✓	✓	×	×	×	✓	×	×	Robust
[31]	✓	✓	×	✓	✓	✓	×	×	Two-stage stochastic
[35]	✓	✓	×	×	×	✓	×	×	Robust
[44]	✓	×	✓	×	×	✓	✓	×	Two-stage stochastic
[36]	✓	×	✓	×	×	✓	×	×	Robust
[39]	✓	✓	×	×	✓	✓	×	×	IGDT
[41]	✓	✓	×	✓	×	✓	×	✓	IGDT
[38]	✓	✓	×	×	×	×	✓	✓	IGDT
Proposed model	✓	×	✓	✓	✓	✓	✓	×	Hybrid IGDT-Stochastic

2. Hybrid IGDT-stochastic AC-TCUC

This paper applies the AC-TCUC problem to investigate the impact of joint operation of DRP and EVPL on power system operating conditions. The proposed model considers the uncertainties of EV owners' behavior and wind power production simultaneously. The uncertainty of EV owners' behavior is modeled through a scenario-based stochastic problem, while the wind power uncertainty is managed using the IGDT approach under a two-level optimization scheme. In the following subsection, the uncertainty of EV owners' behavior is modeled through a scenario-based stochastic problem and problem formulation is presented under a stochastic programming approach, in the next subsection, the presented formulation is modified to a hybrid IGDT-stochastic approach in order to deal with the uncertainty of wind power and EV owners.

2.1. Problem formulation under stochastic programming approach

In this section, the optimization problem is described based on a scenario-based stochastic model. In the following, the objective function and related constraints are explained.

2.1.1. Objective function

In this paper, minimizing power system operating cost by considering AC-calculation for network constraints is the main aim of the provided model. Eq. (1) shows the objective function. The first part states the cost of thermal units' generation including fuel, start-up, and shut-down cost. The second part represents the discharge cost of EVPLs, and the third part defines the cost of consumers' IDRP participation. As it was mentioned before the behavioural uncertainty related to EV owners is modeled using a scenario-based method, and scenario reduction is applied in order to reduce the generated scenarios, so π_s shows the probability of each scenario after scenario reduction.

$$OF_b = \min \sum_{s=1}^{NS} \pi_s \left[\sum_{t=1}^{NT} \left[\begin{array}{l} \sum\limits_{g=1}^{NU} \left(F_g^c(P_{g,t,s}) + SUC_{g,t} + SDC_{g,t} \right) \\ + \sum\limits_{pl=1}^{NPL} \lambda_{pl,t}^{dis} P_{pl,t,s}^{PL2G} + \sum\limits_{j=1}^{NJ_b} \lambda_{j,t} DR_{j,t,s} \end{array} \right] \right] \tag{1}$$

2.1.2. UC constraints

The power production cost of thermal plants which is a quadratic function of the power generation is described in Eq. (2). Start-up/shut down cost should be considered only at the time interval that a unit turned on/off, so a binary variable is introduced in Eqs. (3)-(6) to model this issue [40].

$$F_g^c(P_{g,t,s}) = a_g P_{g,t,s}^2 + b_g P_{g,t,s} + c_g \tag{2}$$

$$SUC_{g,t} \geqslant SU_g \left(Z_{g,t} - Z_{g,t-1} \right) \tag{3}$$

$$SUC_{g,t} \geqslant 0 \tag{4}$$

$$SDC_{g,t} \geqslant SD_g \left(Z_{g,t-1} - Z_{g,t} \right) \tag{5}$$

$$SDC_{g,t} \geqslant 0 \tag{6}$$

Eqs. (7) and (8) shows that each thermal unit should produce active and reactive power within its allowable range. Because boilers and combustion equipment should not be subjected to excessive pressure, the rate of output power change should be limited with ramp up/down limit, this is modeled through (9)-(10) [27].

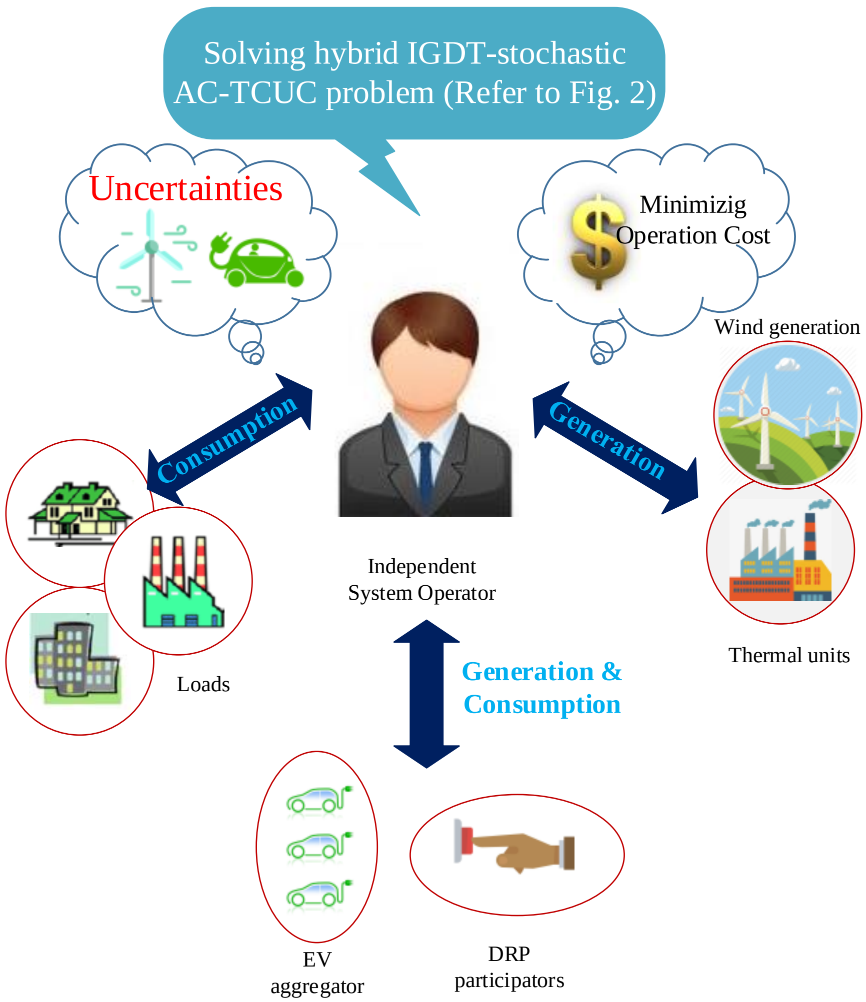

Figure 1: Schematic diagram of the proposed model

It is required for each thermal unit to be online/offline after a start up/shut down for a certain period of time before it shut down/start up which is modeled in (11)-(14) [26].

$$P_g^{\min} Z_{g,t} \leqslant P_{g,t,s} \leqslant P_g^{\max} Z_{g,t} \tag{7}$$

$$Q_g^{\min} Z_{i,t} \leqslant Q_{g,t,s} \leqslant Q_g^{\max} Z_{g,t} \tag{8}$$

$$P_{g,t,s} - P_{g,t-1,s} \leqslant R_g^{up} \tag{9}$$

$$P_{g,t-1,s} - P_{g,t,s} \leqslant R_g^{dn} \tag{10}$$

$$Z_{g,t} - Z_{g,t-1} \leqslant Z_{g,t+TU_{g,u}} \tag{11}$$

$$TU_{g,u} = \begin{cases} u & u \leqslant MUT_g \\ 0 & u > MUT_g \end{cases} \tag{12}$$

$$Z_{g,t-1} - Z_{g,t} \leqslant 1 - Z_{g,t+TD_{g,u}} \tag{13}$$

$$TD_{g,u} = \begin{cases} u & u \leqslant MDT_g \\ 0 & u > MDT_g \end{cases} \tag{14}$$

2.1.3. EVPL constraints

EVs can participate in the energy market via PL operator, in both grid to PL (G2PL) and PL to grid (PL2G) modes. Moreover, EVs can supply reactive power in these two modes. Scenarios of EV owners' behavior are generated according to Eqs. (15)-(18) [28]. In these equations, entry time, exit time, initial state of charge (SOC), and final SOC of each EV are obtained through a scenario generation approach by considering truncated Gaussian distribution. To be sure that generated scenarios are reasonable, Eq. (19) is defined.

$$t_n^{arv} = f_{TG}(\chi; \mu_{arv}, \sigma_{arv}^2, (t_n^{arv,\min}, t_n^{arv,\max})) \tag{15}$$

$$t_n^{dep} = f_{TG}(\chi; \mu_{dep}, \sigma_{dep}^2, (t_n^{dep,\min}, t_n^{dep,\max})) \tag{16}$$

$$SOC_n^{arv} = f_{TG}(\chi; \mu_{SOC_{arv}}, \sigma_{SOC_{arv}}^2, (SOC_n^{arv,\min}, SOC_n^{arv,\max})) \tag{17}$$

$$SOC_n^{dep} = f_{TG}(\chi; \mu_{SOC_{dep}}, \sigma_{SOC_{dep}}^2, (SOC_n^{dep,\min}, SOC_n^{dep,\max})) \tag{18}$$

$$t_n^{arv} \leqslant t_n^{dep} \tag{19}$$

The number of EVs entering or leaving the PL, and the number of EVs that are available in PL at time t, are represented in Eqs. (20)-(22), respectively. Eq. (23) shows that each EVPL has a car capacity that should not be exceeded by EVs which are parked in it. The arrival/ departure of the EVs to/ from the PL affects the total battery capacity of the PL, as represented in Eqs. (24)-(26) [9].

$$N^{arv}_{pl,t,s} = \sum_{t \in t^{dep}_n} N^{EV}_{t^{arv}_n, t^{dep}_n, s} \tag{20}$$

$$N^{dep}_{pl,t,s} = \sum_{t \in t^{arv}_n} N^{EV}_{t^{arv}_n, t^{dep}_n, s} \tag{21}$$

$$N_{pl,t,s} = N_{pl,t-1,s} + N^{arv}_{pl,t,s} - N^{dep}_{pl,t,s} \tag{22}$$

$$N_{pl,t,s} \leqslant N^{max}_{pl} \tag{23}$$

$$Cap^{arv}_{pl,t,s} = \sum_{n=1}^{NEV} \sum_{t \in t^{dep}_n} Cap^{EV}_{n,t^{arv}_n, t^{dep}_n, s} \tag{24}$$

$$Cap^{dep}_{pl,t,s} = \sum_{n=1}^{NEV} \sum_{t \in t^{arv}_n} Cap^{EV}_{n,t^{arv}_n, t^{dep}_n, s} \tag{25}$$

$$Cap_{pl,t,s} = Cap_{pl,t-1,s} + Cap^{arv}_{pl,t,s} - Cap^{dep}_{pl,t,s} \tag{26}$$

Equations (27) and (28) show that the amount of active power that can be exchanged between EVPL and network is capped by the nominal rate of discharging or charging power of EVs and the number of available EVs at the PL [21]. In order to avoid simultaneous PL2G and G2PL modes (29) is considered. As it was mentioned before, reactive power injection potential for the EVPL is considered, and the amount of exchangeable apparent power between EVPL and grid is limited by the PL infrastructure in (30) [24].

$$P^{PL2G}_{pl,t,s} \leqslant \xi^{dis} N_{pl,t,s} P^{max}_{pl} U^{PL2G}_{pl,t,s} \tag{27}$$

$$P^{G2PL}_{pl,t,s} \leqslant \xi^{ch} N_{pl,t,s} P^{max}_{pl} U^{G2PL}_{pl,\ t,s} \tag{28}$$

$$U^{PL2G}_{pl,t,s} + U^{G2PL}_{pl,t,s} \leqslant 1 \tag{29}$$

$$\left(P^{PL2G}_{pl,t,s} + P^{G2PL}_{pl,t,s}\right)^2 + \left(Q^{PL2G}_{pl,t,s} + Q^{G2PL}_{pl,t,s}\right)^2 \leqslant (S^{max}_{pl})^2 \tag{30}$$

The total amount of stored PL energy at time t, increases/decreases as much as SOC of EVs which arrive/ depart to/ from PL at that time. This is illustrated in

Eqs. (31) and (32), respectively [15]. The amount of stored energy in PL at each time can be calculated from EVs entry/exit at that time and parking interaction with the grid in Eq. (33). Since the lifetime of EVs battery can be reduced at very low or very high SOC, (34) defines an allowable range for the SOC of PL.

$$SOE^{arv}_{pl,t,s} = \sum_{n=1}^{NEV} \sum_{t \in t^{dep}_n} Cap^{EV}_{t^{arv}_n, t^{dep}_n, s} SOC^{EV}_{n, t^{arv}_n, t^{dep}_n, s} \tag{31}$$

$$SOE^{dep}_{pl,t,s} = \sum_{n=1}^{NEV} \sum_{t \in t^{arv}_n} Cap^{EV}_{t^{arv}_n, t^{dep}_n, s} SOC^{EV}_{n, t^{arv}_n, t^{dep}_n, s} \tag{32}$$

$$SOE_{pl,t,s} = SOE_{pl,t-1,s} + SOE^{arv}_{pl,t,s} - SOE^{dep}_{pl,t,s} + \eta^{ch} P^{G2PL}_{pl,t,s} - \frac{P^{PL2G}_{pl,t,s}}{\eta^{dis}} \tag{33}$$

$$SOC^{\min}_{pl} Cap_{pl,t,s} \leqslant SOE_{pl,t,s} \leqslant SOC^{\max}_{pl} Cap_{pl,t,s} \tag{34}$$

2.1.4. IDRP constraints

DRPs can be classified into price-based schemes and incentive-based schemes [45]. Participants can shift their consumption from high-demand periods to low-demand periods by taking involved in DRPs. In this paper, IDRP is applied. The amount of load after participating in IDRP and the boundaries for adjustable load are declined in Eqs. (35) and (36) [46]. Eq. (37) illustrates how to implement IDRP on reactive load. Since no electric load should be missed, the summation of the shifted load over the total time horizon must be zero which is illustrated in Eq. (38).

$$D^{r}_{j,t,s} = D_{j,t} - DR_{j,t,s} \tag{35}$$

$$\begin{cases} DR^{\min}_{j} Y_{j,t,s} \leqslant DR_{j,t,s} \leqslant DR^{max}_{j} Y_{j,t,s} & \text{if } DR_{j,t,s} \geqslant 0 \\ DR_{j,t,s} \geqslant D_{j,t} - (1+\gamma) D_{j,t} & else \end{cases} \tag{36}$$

$$Q^{r}_{j,\ t,s} = D^{r}_{j,t,s} \tan(\varphi_j) \tag{37}$$

$$\sum_{t=1}^{NT} DR_{j,t,s} = 0 \tag{38}$$

The rate of load change when participating in a DRP shall not exceed its permissible limit in the consecutive time intervals according to the load structure, so similar to the ramp-up/down limits which have been defined for thermal units, (39) and (40) are defined for DRP participant below.

$$D^{r}_{j,t} - D^{r}_{j,t-1} \leqslant \Delta d^{up}_{j} \tag{39}$$

$$D^{r}_{j,t-1} - D^{r}_{j,t} \leqslant \Delta d^{dn}_{j} \tag{40}$$

Similar to the minimum on/ off times for thermal power plants, in DRPs a specific load is supplied or curtailed in the scheduling horizon. Minimum on time shows the number of sequential time intervals that the load would be supplied after it is restored. Minimum off time represents the minimum number of sequential time intervals that a load would be off after it is curtailed. These are defined by Eqs. (41)-(44).

$$Y_{j,t,s} - Y_{j,t-1,s} \leqslant Y_{j,t+TU_{j,p},s} \tag{41}$$

$$TU_{j,p} = \begin{cases} p & p \leqslant MUT_j \\ 0 & p > MUT_j \end{cases} \tag{42}$$

$$Y_{j,t-1,s} - Y_{j,t,s} \leqslant 1 - Y_{j,t+TD_{j,p},s} \tag{43}$$

$$TD_{j,p} = \begin{cases} p & p \leqslant MDT_j \\ 0 & p > MDT_j \end{cases} \tag{44}$$

2.1.5. AC-network constraints

As it was mentioned before, in this work AC power flow is applied in order to model network constraints. Active and reactive power balance are modeled in (45) and (46), which indicate the total amount of generated active (reactive) power should be equal to consumed active (reactive) power [28]. Voltage magnitude and voltage angle of the system buses should not exceed a predefined value, which is represented in (47) and (48) [44]. Equation (49) shows that the loading limit for a transmission line shall be its thermal loading limit [28].

$$\sum_{g=1}^{NU_b} P_{g,\ t,s} + \sum_{w=1}^{NW_b} \widehat{P}_{w,t} + \sum_{pl=1}^{NPL_b} P^{PL2G}_{pl,\ t,s} - \sum_{pl=1}^{NPL_b} P^{G2PL}_{pl,\ t,s} - \sum_{j=1}^{NJ_b} D^{r}_{j,t,s} = \sum_{l=1}^{NL_b} PF_{l,\ t,s} \tag{45}$$

$$\sum_{g=1}^{NU_b} Q_{g,\ t,s} + \sum_{w=1}^{NW_b} \widehat{Q}_{w,t} - \sum_{pl=1}^{NPL_b} Q_{pl,\ t,s} - \sum_{j=1}^{NJ_b} Q^{r}_{j,\ t,s} = \sum_{l=1}^{NL_b} QF_{l,\ t,s} \tag{46}$$

$$V^{min}_{b} \leqslant V_{b,t,s} \leqslant V^{max}_{b} \tag{47}$$

$$\delta_b^{min} \leqslant \delta_{b,t,s} \leqslant \delta_b^{max} \tag{48}$$

$$PF_{l,\ t,s}^2 + QF_{l,\ t,s}^2 \leqslant (S_l^{max})^2 \tag{49}$$

Active and reactive power flow of line l that connects bus b to b' are demonstrated in (50) and (51) which are a function of the line impedance and the voltage of the two connecting buses [36].

$$PF_{l,\ t,s} = \frac{V_{b,t,s}^2}{Z_l}\cos(\theta_L) - \frac{V_{b,t,s}V_{b',t,s}}{Z_l}\cos(\delta_{b,t,s} - \delta_{b',t,s} + \theta_l) \tag{50}$$

$$QF_{l,\ t,s} = \frac{V_{b,t,s}^2}{Z_l}\sin(\theta_L) - \frac{V_{b,t,s}V_{b',t,s}}{Z_l}\sin(\delta_{b,t,s} - \delta_{b',t,s} + \theta_l) \tag{51}$$

2.2. Applying IGDT approach in stochastic programming problem

IGDT is a high-performance method to deal with severe uncertain parameters. Since there is no need for the production of a large number of scenarios in IGDT, the problem-solving time is much lower than scenario-based programming. Moreover, IGDT does not need the PDF for uncertain parameters. Compared to the robust optimization method that considers the uncertainty radius of the uncertain parameters as a predefined value, it is not needed to be known when employing IGDT method. In fact, the main objective of solving the optimization problem in the proposed model is determining the forecast error of the uncertain parameter from its forecasted value. In this paper, IGDT is applied to deal with uncertainty related to wind power production. Among different uncertain parameters models, the envelope bound model is applied to show the prior knowledge about the uncertain parameters Ψ, such as Eq. (52) [39].

$$U = U(\overline{\Psi},\ \varepsilon) = \left\{\Psi : \left|\frac{\Psi - \overline{\Psi}}{\overline{\Psi}}\right| \leqslant \varepsilon\right\} \tag{52}$$

In the proposed model both RA and RS strategies are considered which is illustrated in Figure 2. The mathematical formulation of these strategies is presented in the next two subsections.

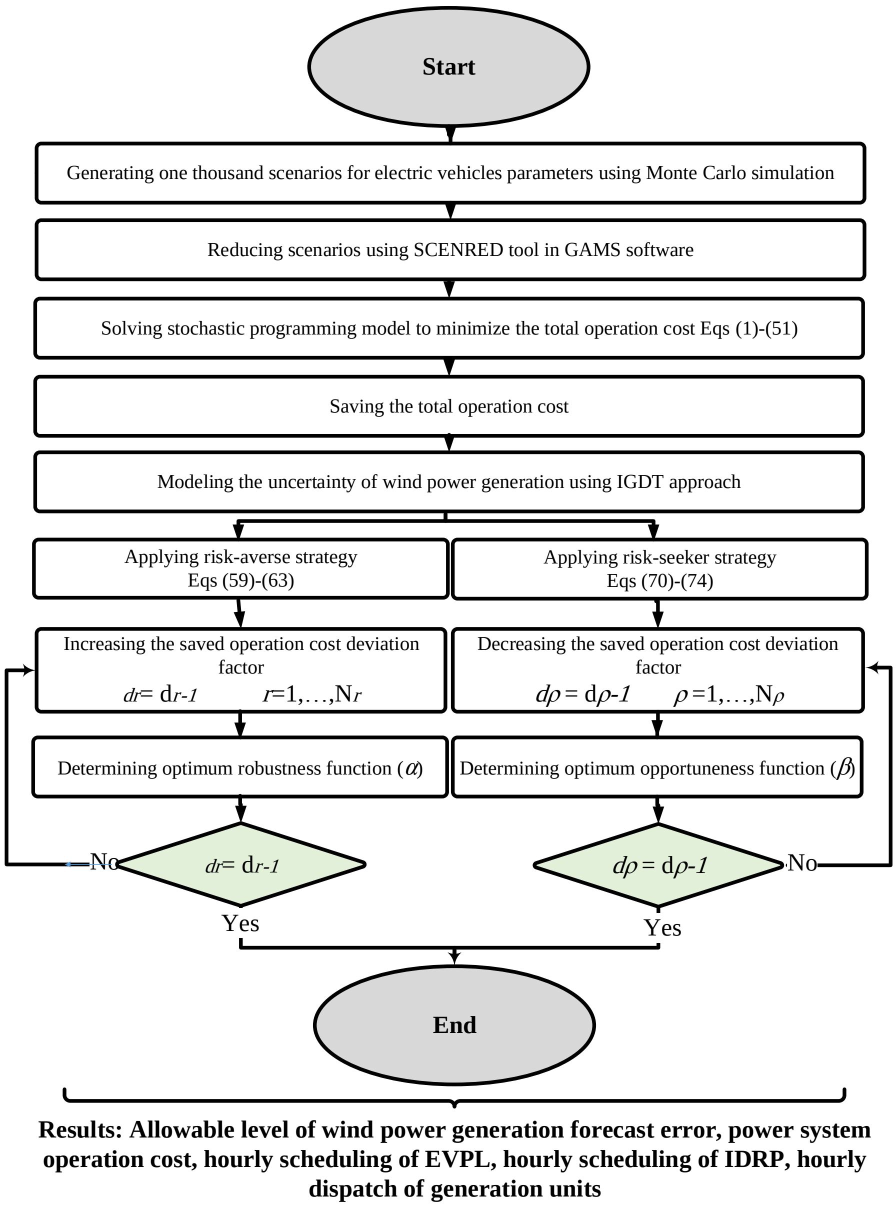

Figure 2: Flowchart of the proposed hybrid IGDT-stochastic approach

2.2.1. *RA strategy*

In this strategy, the undesirable impact of the uncertain parameter on the objective function is considered. The RA attitude aim is to overcome the incremental of operation cost that is caused by the undesirable variation of wind generation from its forecasted value. The mathematical formula of the RA strategy in IGDT approach is represented bellow [47].

$$\alpha(X, \Delta^r) = \mathrm{Max}\left\{\varepsilon : \left(\underset{\Psi \in U(\bar{\Psi}, \varepsilon)}{\mathrm{Max}} \quad OF \leqslant \Delta^r = (1 + d_r) OF_b\right)\right\} \tag{53}$$

The main goal of applying IGDT approach for the ISO is to maximize the uncertain parameter radius which is modeled as a two-level problem in Eqs. (54)-(58) [39]. In this model, the uncertain radius of the uncertain parameter is maximized in the first level and expected operation cost is minimized in the second level.

$$\alpha = \max \quad \varepsilon \tag{54}$$

subject to:

$$\mathrm{Max} \sum_{s=1}^{NS} \pi_s \left[\sum_{t=1}^{NT} \left[\begin{array}{l} \sum\limits_{g=1}^{NU} \left(F_g^c(P_{g,\,t,s}) + SUC_{g,\,t} + SDC_{g,\,t} \right) \\ + \sum\limits_{pl=1}^{NPL} \lambda_{pl,t}^{dis} P_{pl,t,s}^{dis} + \sum\limits_{j=1}^{NJ_b} \lambda_{j,t} DR_{j,t,s} \end{array} \right] \right] \leqslant \Delta^r \tag{55}$$

$$\Delta^r \leqslant (1 + d_r) OF_b \tag{56}$$

$$(1 - \varepsilon)\widehat{P}_{w,t} \leqslant P_{W,t} \leqslant (1 + \varepsilon)\widehat{P}_{w,t} \tag{57}$$

$$\mathrm{Eqs.}\ (2) - (51) \tag{58}$$

Because of the complexity of solving a two-level optimization problem through common optimization software, the provided two-level model in Eqs. (54)-(58) is converted to a single-level problem as demonstrated in Eqs. (59)-(63).

$$\alpha = \max \quad \varepsilon \tag{59}$$

$$\mathrm{sum}_{s=1}^{NS} \pi_s \left[\sum_{t=1}^{NT} \left[\begin{array}{l} \sum\limits_{g=1}^{NU} \left(F_g^c(P_{g,\,t,s}) + SUC_{g,\,t} + SDC_{g,\,t} \right) \\ + \sum\limits_{pl=1}^{NPL} \lambda_{pl,t}^{dis} P_{pl,t,s}^{dis} + \sum\limits_{j=1}^{NJ_b} \lambda_{j,t} DR_{j,t,s} \end{array} \right] \right] \leqslant \Delta^r \tag{60}$$

$$\Delta^r \leqslant (1 + d_r) OF_b \tag{61}$$

$$P_{W,t} = (1 - \varepsilon)\widehat{p}_{w,t} \tag{62}$$

$$\mathrm{Eqs.}\ (2) - (51) \tag{63}$$

2.2.2. RS strategy

It is worthwhile to say that sometimes violation of the uncertain parameter from its forecasted amount has a favorable impact on the objective function. An RS strategy is represented in this situation. As a matter of fact, the ISO goal is to decline the objective function more than the basic condition value. The mathematical model for the RS strategy is described as Eq. (64) [47]:

$$\beta(X, \Delta^{\rho}) = \mathrm{Min}\left\{\varepsilon : \left(\underset{\Psi\in U(\bar{\Psi},\varepsilon)}{\mathrm{Min}} \ OF \leqslant \Delta^{\rho} = (1-d_{\rho})OF_{b}\right)\right\} \tag{64}$$

This strategy can be formulated as a two-level optimization in which the uncertain radius of the uncertain parameter is minimized in the first level and expected operation cost is minimized in the second level as it is illustrated in (65)-(69) [43].

$$\beta = \min \varepsilon \tag{65}$$

$$\mathrm{Min}\sum_{s=1}^{NS}\pi_s\left[\sum_{t=1}^{NT}\left[\begin{array}{l}\sum\limits_{g=1}^{NU}\left(F_g^c(P_{g,\,t,s}) + SUC_{g,\,t} + SDC_{g,\,t}\right)\\ +\sum\limits_{pl=1}^{NPL}\lambda_{pl,t}^{dis}P_{pl,t,s}^{dis} + \sum\limits_{j=1}^{NJ_b}\lambda_{j,t}DR_{j,t,s}\end{array}\right]\right] \leqslant \Delta^{\rho} \tag{66}$$

subject to:

$$\Delta^{\rho} \leqslant (1-d_p)OF_b \tag{67}$$

$$(1-\varepsilon)\widehat{P}_{w,t} \leqslant P_{W,t} \leqslant (1+\varepsilon)\widehat{P}_{w,t} \tag{68}$$

$$\mathrm{Eqs.}\ (2)-(51) \tag{69}$$

As mentioned before, the increase in wind power generation provides a desirable impact on the operation cost. Therefore, in the proposed RS attitude, the minimum operation cost is obtained when wind generation rises from the predicted amount. The single-level problem in Eqs. (70)-(74) can be presented instead of the proposed two-level model in Eqs. (65)-(69) :

$$\beta = \min \varepsilon \tag{70}$$

$$\sum_{s=1}^{NS}\pi_s\left[\sum_{t=1}^{NT}\left[\begin{array}{l}\sum\limits_{g=1}^{NU}\left(F_g^c(P_{g,\,t,s}) + SUC_{g,\,t} + SDC_{g,\,t}\right)\\ +\sum\limits_{pl=1}^{NPL}\lambda_{pl,t}^{dis}P_{pl,t,s}^{dis} + \sum\limits_{j=1}^{NJ_b}\lambda_{j,t}DR_{j,t,s}\end{array}\right]\right] \leqslant \Delta^{\rho} \tag{71}$$

$$\Delta^{\rho} \leqslant (1-d_p)OF_b \tag{72}$$

$$P_{w,t} = (1+\varepsilon)\widehat{p}_{w,t} \tag{73}$$

$$\text{Eqs. } (2) - (51) \tag{74}$$

3. Numerical studies

To evaluate the effectiveness of the presented model, it is implemented on a modified six-bus system, which is illustrated in Figure 3. This system contains seven lines, three thermal generation units, three loads, one wind farm, and one EVPL. Table 2 shows technical characteristics of the system lines [48]. The thermal units operating cost coefficients and the technical characteristics are represented in Table 3. It is worthwhile to say that according to these cost coefficients, unit G2 is the most costly unit and unit G1 is the cheapest unit. The information about the predicted wind power production and load is shown in Figure 4 [40]. The specifications of EVs for evaluating the impact of EVPLs on system operation conditions are summarized in Table 4 [9]. It is assumed that the desired state of charge of each EV at departure time is more than 70% and so the main purpose of EV owners that is charging their EV battery will be satisfied. The cost of load participation in DRP and discharge cost for EVPL is considered 5 $/MWh. In order to model the uncertain behavior of EV owners, a thousand scenarios are generated using the Monte Carlo simulation approach, which is reduced to five scenarios applying a fast-backward approach. The proposed model is a mixed-integer non-linear problem (MINLP) which is solved by discrete and continuous optimizer (DICOPT) solver in general algebraic modeling system (GAMS) environment containing 1752 single variables and 3057 single equations. GAMS is a high-level modeling system appropriate for modeling and solving mathematical problems and non-convex optimization. Solutions resulted from DICOPT can be globally optimal with a fair degree of confidence, so that it has been utilized in some literature such as [8, 27, 37, 41, 49–51]. DICOPT solves the MINLP problem via a series of NLP and MIP sub-problems. These sub-problems are solved using CONOPT and CPLEX solver, respectively. Figure 5 shows the flowchart for the related solution algorithm.

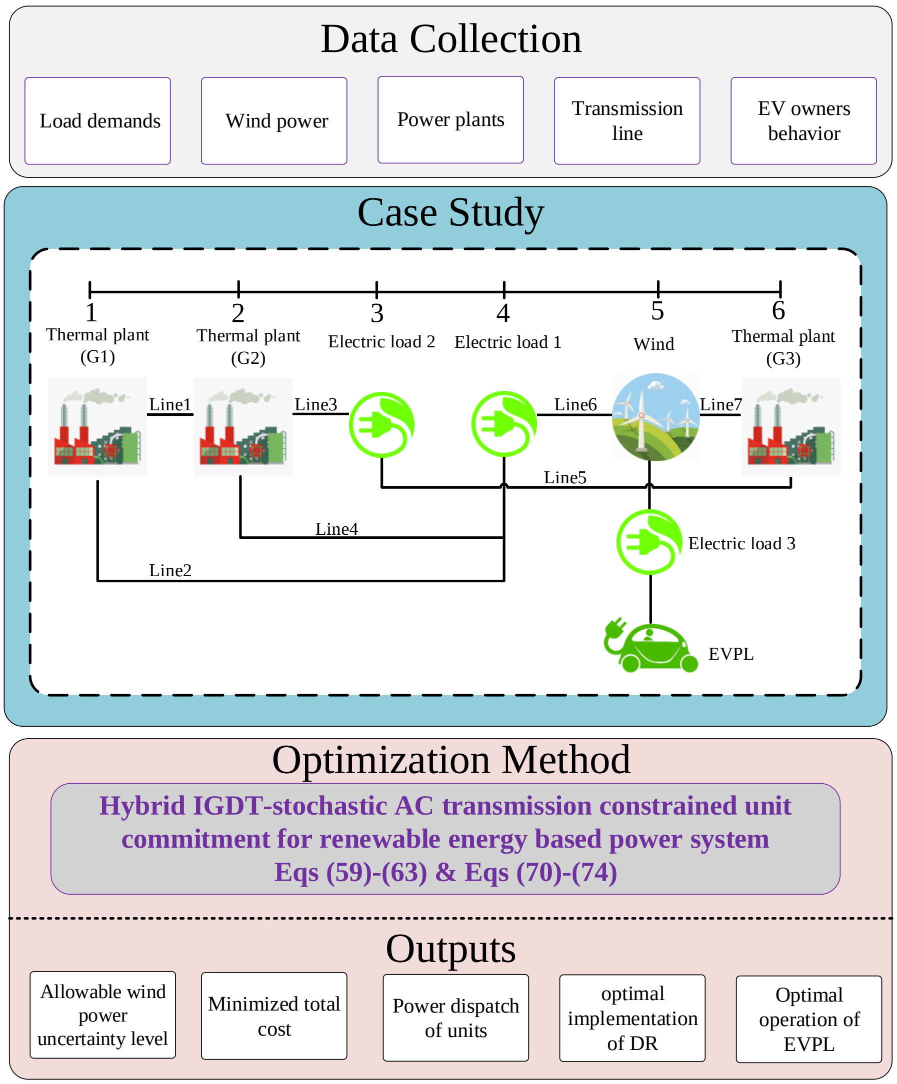

Figure 3: Schematic diagram of the studied case study

Table 2: Technical characteristics of the lines

Line number	Starting bus	End bus	R (pu)	X (pu)	S_{max} (MVA)
1	1	2	0.005	0.170	200
2	1	4	0.003	0.258	100
3	2	3	0.000	0.037	100
4	2	4	0.007	0.197	100
5	3	6	0.000	0.018	100
6	4	5	0.000	0.037	100
7	5	6	0.002	0.140	100

Table 3: Cost coefficients and technical characteristics of the thermal units

	a ($/MW^2)	b ($/MW)	c ($/h)	P_{min} (MW)	P_{max} (MW)	Q_{min} (MVar)	Q_{max} (MVar)	R^{up} (MW/h)	R^{dn} (MW/h)	MUT (h)	MDT (h)
G1	0.0004	13.51	176.95	100	220	-80	200	55	55	4	4
G2	0.001	35.63	129.97	10	100	-40	70	50	50	2	3
G3	0.005	17.7	137.41	10	20	-40	50	20	20	1	1

The effectiveness of the provided model are examined by implementing following cases:

Case study 1 (<u>CS1</u>): Stochastic AC-TCUC problem considering EVPL.

Case study 2 (<u>CS2</u>): Stochastic AC-TCUC problem considering EVPL and DRP.

Case study 3 (<u>CS3</u>): Applying IGDT approach in AC-TCUC problem

<u>CS1</u>: Stochastic AC-TCUC problem considering EVPL

In this case, an electric vehicle parking lot is considered at bus 5 and the application of DRPs is not considered. In order to clarify the effectiveness of EVPL capabilities on expected operating cost reduction, it is assumed that EVPL acts as a passive load at first. It means that no reactive power is injected into the grid by the parking lot and it only works in G2PL mode. By implementing the proposed model, the expected operating cost equals $75,895.36, which is $276.67 more than when there is no EVPL in the grid. It is due to an increase in grid load by considering EVPL. The expected power dispatch of units is shown in Figure 6. Since unit G1 is the cheapest unit, it is committed over the whole day while unit G2 as the most

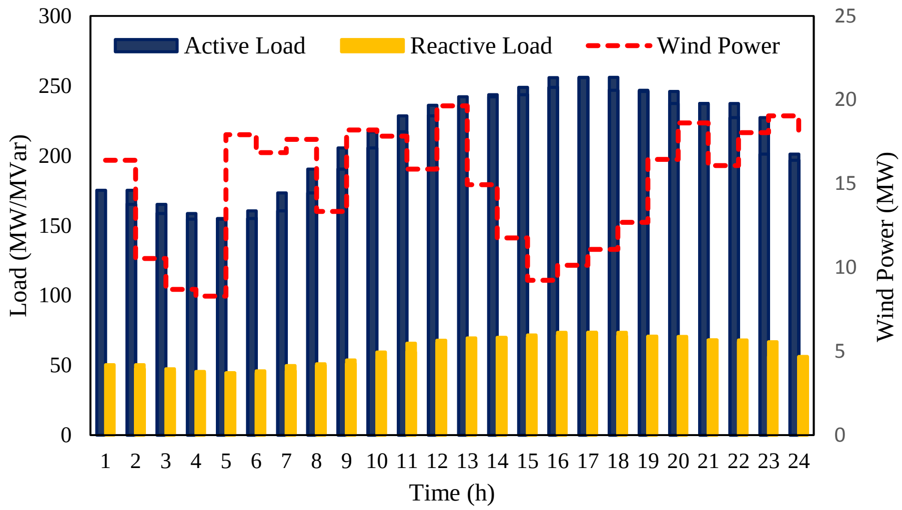

Figure 4: Predicted wind power production and load demand

Table 4: Technical characteristics of EVs

$\zeta^{dis/ch}$ (kW/h)	$\eta^{dis/ch}$ (%)	SOC_{pl}^{min} (%)	SOC_{pl}^{max} (%)	Capacity (kWh)
11	90	30	90	20

costly unit is committed only for 8 hours. Although the demand for electricity is more than the maximum power output of the unit G1 at peak period, this unit is not operating at its maximum value at high demand hours. This is because of the thermal capacity limitation of the lines connected to unit G1. In the next step, active power injection capability is considered for the parking lot, which means that it can operate in both G2PL and PL2G modes. Figure 7 shows the scheduling of the parking lot. It can be seen that in the off-peak period, EVPL is in the G2PL mode in order to address two goals; charging EVs battery to the desired SOC, and storing energy in order to answer the power need of grid at high demand period. At the same time, it is in PL2G mode over peak period and sells its energy to the grid. This interaction leads to \$149.30 cost saving in comparison with when no EVPL is in the grid (the expected operating cost equals \$75,469.39 in this situation). Figure 8 shows the power flow in line 2. As illustrated in this figure, line 2 which is con-

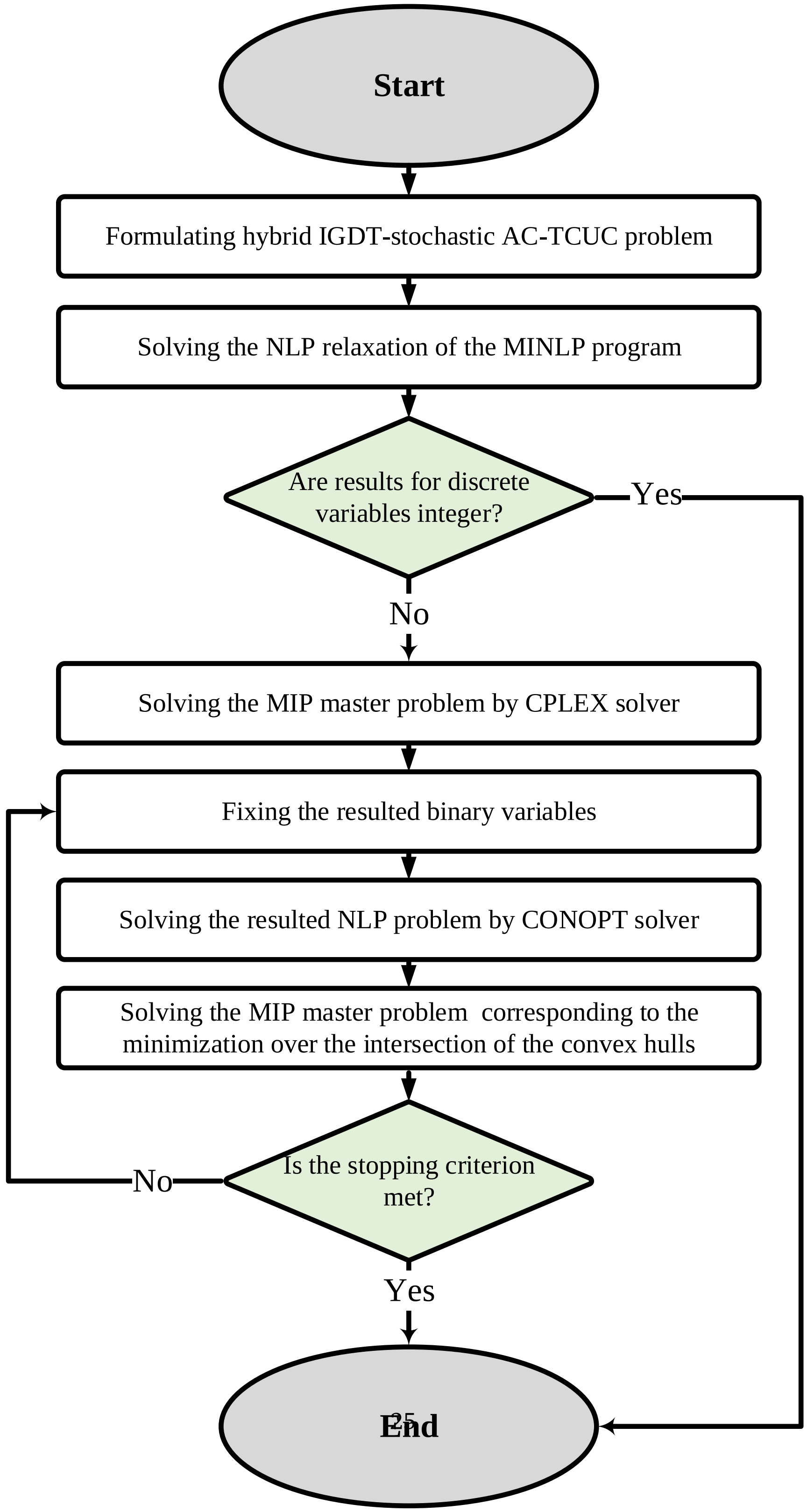

Figure 5: Flowchart of DICOPT algorithm for solving MINLP

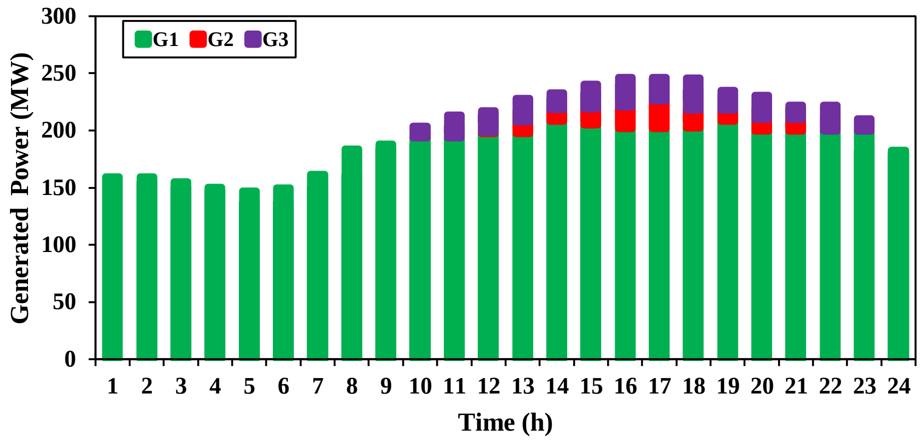

Figure 6: Expected power dispatch of thermal units

nected to the cheapest unit, operates at its maximum thermal capacity (100MVA) most of the time during a day. That is why more utilization from unit G1 is not possible. The potential of reactive power injection by EVPL can compensate reactive power flow of power lines and so more line capacity will be allocated to active power. As a consequence, unit G1 is able to provide more active power and it provides more cost-saving for the ISO. The effect of reactive power injection capability of EVPL on the active and reactive power flow of line 2 is illustrated in Figures 9 and 10, respectively. Improving EVPL operation by considering reactive power injection leads to the expected operating cost of $74,707.56, which is $911.13 lesser than the situation without EVPL. Table 5 easily compares system operating cost and power generation of thermal plants in two case of with and without reactive power injection for EVPL.

Table 5: Expected operation cost and units' dispatch with and without reactive power injection for EVPL

	Operation cost ($)	G_1(MWh)	G_2(MWh)	G_3(MWh)
EVPL without Q injection	75469.39	4441.01	166.25	188.25
EVPL with Q injection	74707.56	4473.79	96.16	175.48

<u>CS2</u>: Stochastic AC-TCUC problem considering EVPL and DRP

In this case, the impact of both DRP and EVPL on power system operating cost

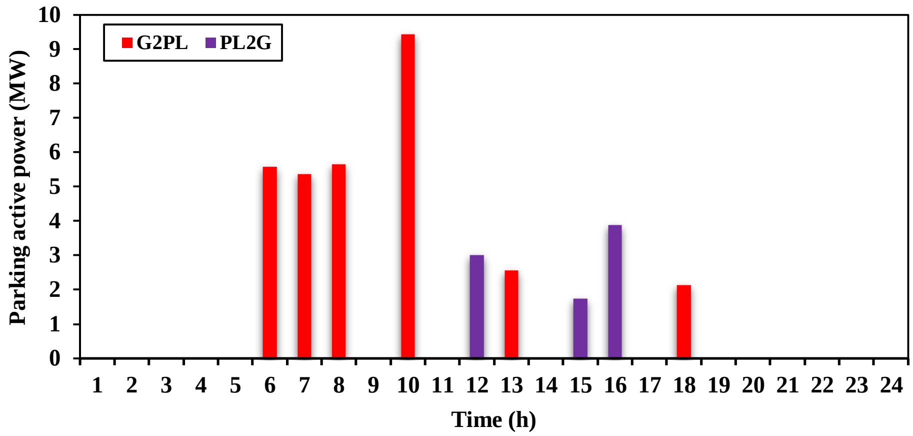

Figure 7: Expected scheduling of EVPL

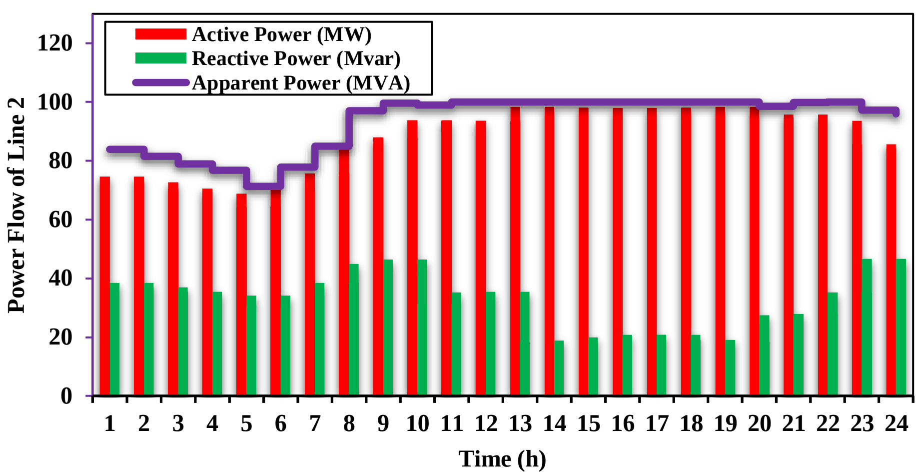

Figure 8: Power flow of line 2 without considering reactive power injection for EVPL

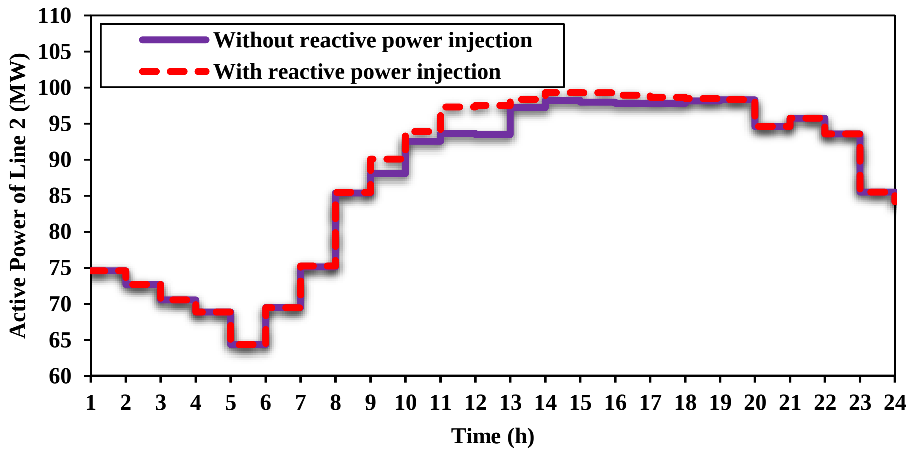

Figure 9: The impact of reactive power injection of EVPL on the active power flow of line 2

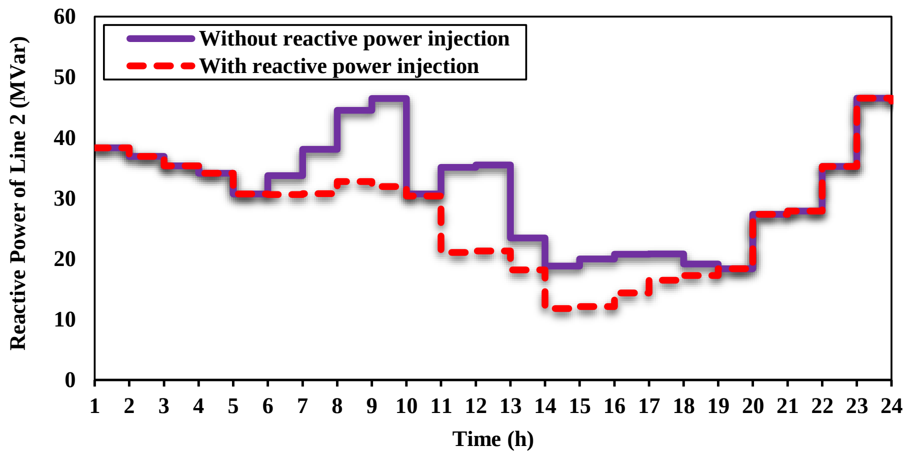

Figure 10: The impact of reactive power injection of EVPL on the reactive power flow of line 2

and thermal unit dispatch are evaluated. A participation factor of 3% is considered for DRP. Figure 11 shows active and reactive load profile before and after participating in DRP. By implementing DRP, participants shift their active and reactive load from high demand period to low demand period according to the DR participant factor, so the need for power in the on-peak period decreases. As a consequence the expected power dispatch of the most costly unit G2, and the expected operating cost will decline. This leads to the operating cost of $73,486.85 which is $1220.71 less than the previous case. This reduction illustrates the effectiveness of the simultaneous operation of EVPL and DRP on cost-saving. Figure 12 illustrates the expected power dispatch of the unit G1 and G2 for DR participation factor of 3% and 7%. As can be seen by increasing consumers' participation in DRP, the need for producing power by the unit G2 in the high demand period decreases. In consequence this unit is committed only for 2 hours. Table 6 illustrates the change of expected operating cost and power dispatch of thermal plants relative to DR participation factor. It can be seen that the expected operating cost declines by the increment of DR participation factor. This trend continues until when DR participation factor reaches the amount of 16%. After that no cost-saving will be achieved since the generation of unit G1 reaches its maximum limit, and the last two rows of the table show no improvement in terms of cost savings.

CS3: Hybrid IGDT-stochastic AC-TCUC problem

In this case, the wind power uncertainty is modeled using the IGDT approach. In order to evaluate the impact of EVPL and DRP on range of manageable wind power uncertainty, this approach is implemented in both previous cases as well as the case in which none of EVPL and DRP is incorporated in the system. The expected operating cost of the latter is considered as the base condition operating cost which equals $75618.69. The RA strategy is implemented by raising the robustness parameter d_r from 0.005 to 0.050 with steps of 0.005. Figure 13 shows the direct relationship between robustness function and robustness parameter for all three aforementioned cases. It means that as d_r (and consequently operating cost) increases ISO can manage a larger amount of wind power uncertainty. For example, in the presence of EVPL and DRP for d_r= 0.005 (0.5% increment in operating cost) the amount

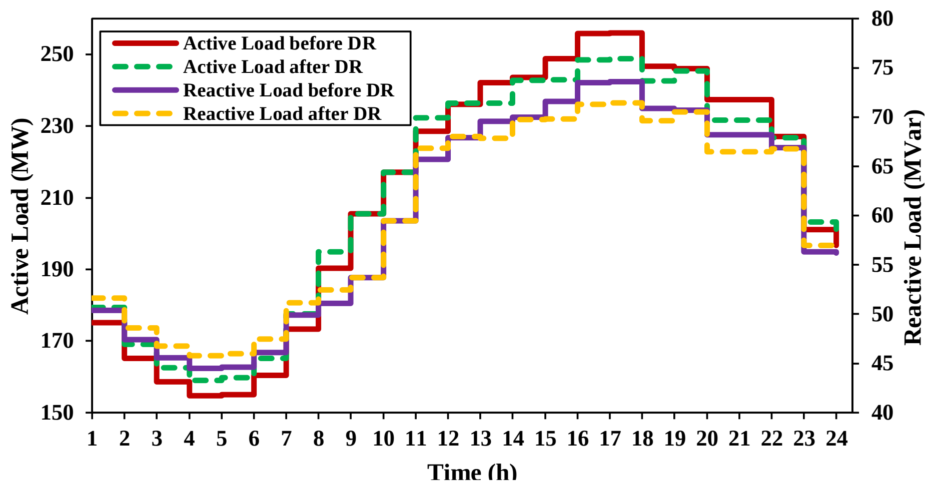

Figure 11: Active and reactive load profile before and after DR participation

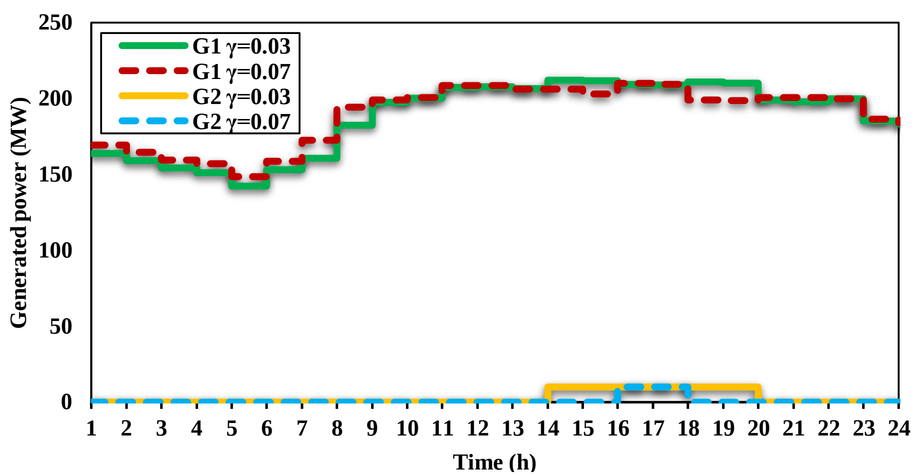

Figure 12: The impact of DR on the expected power dispatch of units G1 and G2

Table 6: Expected operation cost and units generation for different DR participation factor

DR participation factor (%)	Operation cost ($)	G_1(MWh)	G_2(MWh)	G_3(MWh)
1	74492.05	4494.13	84.64	166.29
3	73486.85	4521.36	50.00	172.27
5	73230.21	4545.01	40.00	160.10
7	72697.42	4545.23	20.00	178.70
9	72017.52	4571.90	0.00	172.03
11	71951.68	4584.31	0.00	159.61
13	71927.42	4595.10	0.00	148.60
15	71907.99	4622.50	0.00	121.42
17	71905.51	4623.93	0.00	120.00
19	71905.51	4623.93	0.00	120.00

of α equals to 0.29 which means that 29% error in forecasted wind power can be covered, while for $d_r = 0.015$, robustness function is 0.38 meaning that a more extensive range of the wind power uncertainty is acceptable but with the higher operating cost. Comparing three curves in Figure 13 depicts that incorporating EVPL and DRP in the system benefits ISO in terms of wind uncertainty handling since by the same amount of cost increase a wider range of wind generation uncertainty can be managed. For instance by 3% rise in cost only 21% of wind uncertainty can be addressed in the absence of EVPL and DRP while the equivalent figures for CS1 and CS2 are 34% and 50%, respectively. Figure 14 shows how the power dispatch of units G1 and G2 change when α increases. It illustrates that by increasing manageable amount of wind power uncertainty, generation of thermal units especially the most costly unit (G2) rises such that the difference between wind power generation and its predicted value can be compensated by thermal generation. To implement RS strategy, the opportunity parameter d_ρ is increased from 0.005 to 0.050 with steps of 0.005. This resulted in an operating cost reduction compared to its value in the base condition. It can be seen in Figure 15 that there is a direct relation between opportunity parameter and the opportuneness function β. This means that as more optimistic operation cost reduction is desired, more increment in wind power gen-

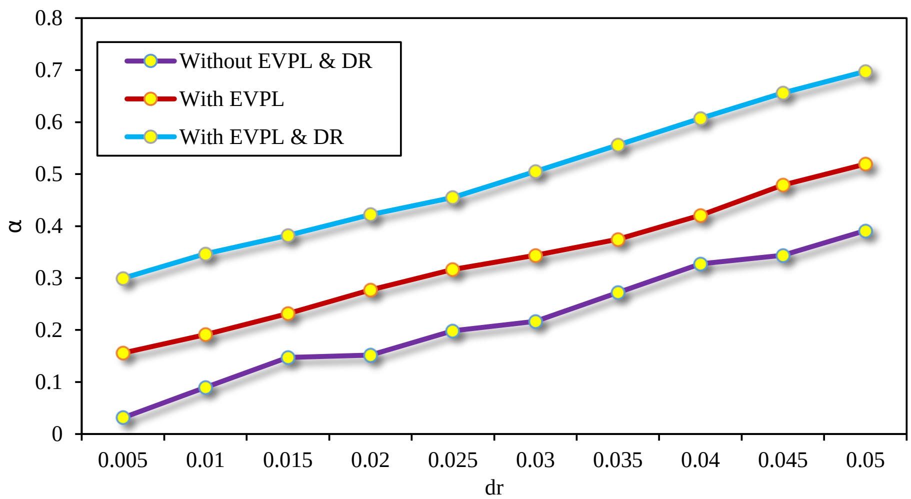

Figure 13: Change of robustness function relative to robustness parameter

eration compared to its predicted value is needed. For example, in the presence of EVPL and DRP, when $d_\rho = 0.045$ (i.e. 4.5% desirable operating cost reduction) the amount of β is 0.07 (7% error in forecasted wind power is needed) while for $d_\rho = 0.05$, opportuneness function is 0.17. It is also worthwhile to say that incorporating EVPL and DRP in the power system diminishes the need for a wide range of optimistic forecast errors in exchange for a distinct amount of cost reduction. This is because of the flexibility that EVPL and DRP provide for the ISO. For instance, in exchange of 4% fall in operation cost, there is no need for any forecasted error in wind generation by considering EVPL and DRP in the system, since the impact of EVPL and DRP already prepared this cost reduction. Whereas in the absence of EVPL and DRP 40%, optimistic error is needed.

4. Conclusion

In this paper, the impact of coordinated utilization of EVPL and IDRP on power system operating condition has been investigated under an AC-TCUC framework. Wind power uncertainty was modeled by applying IGDT approach under both RA and RS strategies which facilitate decision making for ISO with higher reliability. A scenario-based approach using Monte Carlo simulation was implemented in order

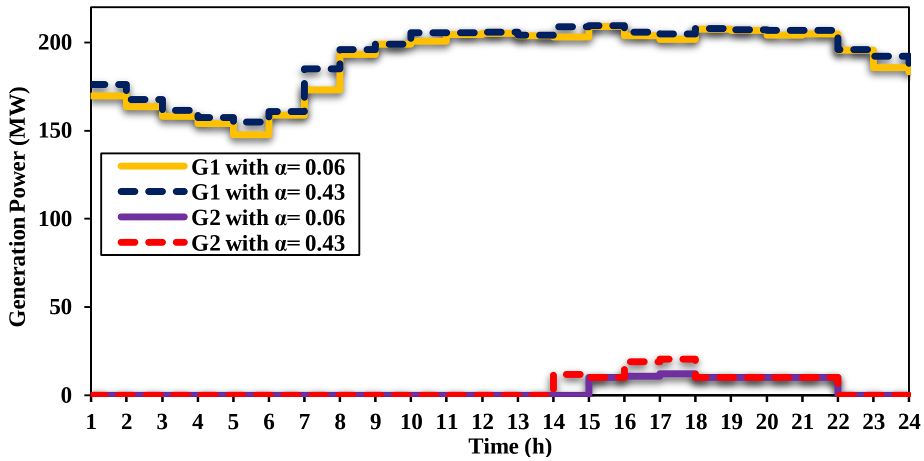

Figure 14: The impact of the robustness function on the expected power dispatch of thermal units

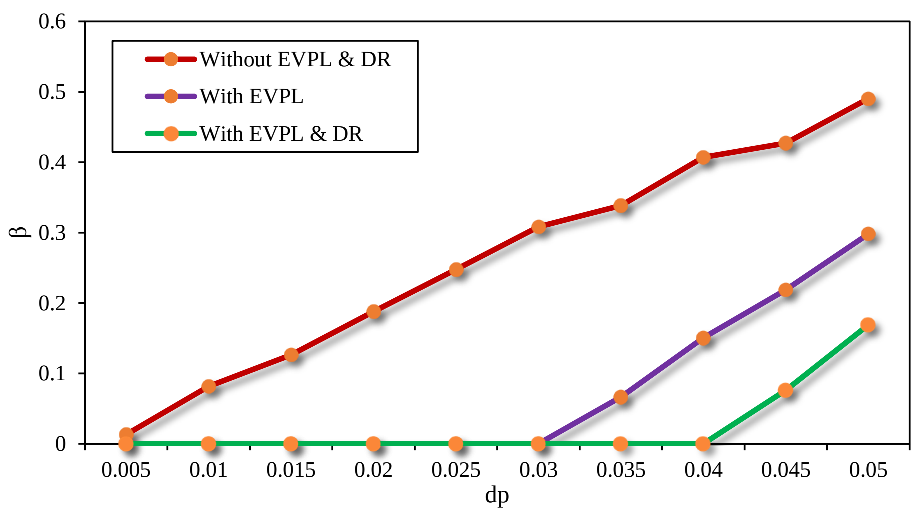

Figure 15: Change of opportuneness function relative to opportunity parameter

to model uncertainties related to EV owners' behavior. Developing a framework for reactive power injection by EVPL and implementing IDRP on both active and reactive power of consumers led to more cost saving and brought the model closer to the reality in comparison with the prior literature. Moreover coordinated utilization of EVPL and IDRP made ISO less vulnerable in terms of handling uncertainties related to power system parameter. The flexibility provided by coordinated scheduling of EVPL and IDRP made more range of wind power uncertainty tolerable for the system. The proposed framework was implemented in the AC-TCUC problem by considering technical requirements related to power system, EVs and participating loads in DRP. In order to make the model more realistic, desires of EV owners and DRP attendees was considered by taking favorable departure SOC and DRP load participation factor into account.Evaluating of the proposed model illustrates some remarkable results in the utilization of smart technologies in terms of cost-saving and RESs uncertainty handling as follows:

- ✓ The joint operation of EVPL and IDRP resulted in a 3.7% reduction in daily operation cost in comparison with the non-coordinated scheduling of these technologies.
- ✓ Reactive power injection capability for EVPL made the utilization of wind power more efficient. This resulted in 1% of more operation cost decrement.
- ✓ Increasing DRP participation factor from 1% to 15% led to a rise in operation cost saving from 1.5% to 5% in the presence of EVPL.
- ✓ Simultaneous operation of EVPL and IDRP in both strategies of RS and RA provided more flexible managing conditions for ISO to cover wind power uncertainty. This boosted the average robustness function from 22% to 49%.

References

[1] U. EPA, Sources of Greenhouse Gas Emissions, https://www.epa.gov/ghgemissions/sources-greenhouse-gas-emissions, [Online; accessed 19-July-2018] (2018).

[2] M. Nazari-Heris, M. A. Mirzaei, B. Mohammadi-Ivatloo, M. Marzband,

S. Asadi, Economic-environmental effect of power to gas technology in coupled electricity and gas systems with price-responsive shiftable loads, Journal of Cleaner Production 244 (2020) 118769.

[3] E. Yao, T. Liu, T. Lu, Y. Yang, Optimization of electric vehicle scheduling with multiple vehicle types in public transport, Sustainable Cities and Society 52 (2020) 101862.

[4] S. Nojavan, M. Majidi, A. Najafi-Ghalelou, M. Ghahramani, K. Zare, A cost-emission model for fuel cell/pv/battery hybrid energy system in the presence of demand response program: ε-constraint method and fuzzy satisfying approach, Energy Conversion and Management 138 (2017) 383–392.

[5] H. Shahinzadeh, J. Moradi, G. B. Gharehpetian, H. Nafisi, M. Abedi, Iot architecture for smart grids, in: 2019 International Conference on Protection and Automation of Power System (IPAPS), 2019, pp. 22–30.

[6] C. Brunner, G. Deac, S. Braun, C. Zöphel, The future need for flexibility and the impact of fluctuating renewable power generation, Renewable Energy 149 (2020) 1314–24.

[7] M. A. Mirzaei, A. S. Yazdankhah, B. Mohammadi-Ivatloo, M. Marzband, M. Shafie-khah, J. P. Catalão, Stochastic network-constrained co-optimization of energy and reserve products in renewable energy integrated power and gas networks with energy storage system, Journal of Cleaner Production 223 (2019) 747–758.

[8] M. Ahrabi, M. Abedi, H. Nafisi, M. A. Mirzaei, B. Mohammadi-Ivatloo, M. Marzband, Robust transmission-constrained ac unit commitment in presence of smart technologies, in: 2019 Smart Grid Conference (SGC), 2019, pp. 1–6.

[9] E. Heydarian-Forushani, M. Golshan, P. Siano, Evaluating the benefits of coordinated emerging flexible resources in electricity markets, Applied Energy 199 (2017) 142–154.

[10] M. Ghahramani, M. Nazari-Heris, K. Zare, B. Mohammadi-ivatloo, Optimal energy and reserve management of the electric vehicles aggregator in electrical energy networks considering distributed energy sources and demand side management, in: Electric Vehicles in Energy Systems, Springer, 2020, pp. 211–231.

[11] R. Razipour, S.-M. Moghaddas-Tafreshi, P. Farhadi, Optimal management of electric vehicles in an intelligent parking lot in the presence of hydrogen storage system, Journal of Energy Storage 22 (2019) 144–152.

[12] O. Hafez, K. Bhattacharya, Integrating ev charging stations as smart loads for demand response provisions in distribution systems, IEEE Transactions on Smart Grid 9 (2) (2018) 1096–1106.

[13] M. Ghahramani, M. Nazari-Heris, K. Zare, B. Mohammadi-Ivatloo, Energy and reserve management of a smart distribution system by incorporating responsive-loads/battery/wind turbines considering uncertain parameters, Energy 183 (2019) 205–219.

[14] M. Shahbazitabar, H. Abdi, A novel priority-based stochastic unit commitment considering renewable energy sources and parking lot cooperation, Energy 161 (2018) 308–324.

[15] M. Shafie-khah, P. Siano, D. Z. Fitiwi, N. Mahmoudi, J. Catalao, An innovative two-level model for electric vehicle parking lots in distribution systems with renewable energy, in: 2018 IEEE Power Energy Society General Meeting (PESGM), 2018, pp. 1–1.

[16] Z. Liu, Q. Wu, S. Huang, L. Wang, M. Shahidehpour, Y. Xue, Optimal day-ahead charging scheduling of electric vehicles through an aggregative game model, IEEE Transactions on Smart Grid 9 (5) (2018) 5173–5184.

[17] G. Wenzel, M. Negrete-Pincetic, D. E. Olivares, J. MacDonald, D. S. Callaway, Real-time charging strategies for an electric vehicle aggregator to provide ancillary services, IEEE Transactions on Smart Grid 9 (5) (2018) 5141–5151.

[18] S. M. B. Sadati], J. Moshtagh, M. Shafie-khah, A. Rastgou, J. P. Cataláo, Operational scheduling of a smart distribution system considering electric vehicles parking lot: A bi-level approach, International Journal of Electrical Power Energy Systems 105 (2019) 159–178.

[19] M.-W. Tian, S.-R. Yan, X.-X. Tian, M. Kazemi, S. Nojavan, K. Jermsittiparsert, Risk-involved stochastic scheduling of plug-in electric vehicles aggregator in day-ahead and reserve markets using downside risk constraints method, Sustainable Cities and Society 55 (2020) 102051.

[20] A. Alahyari, M. Ehsan, M. Mousavizadeh, A hybrid storage-wind virtual power plant (vpp) participation in the electricity markets: A self-scheduling optimization considering price, renewable generation, and electric vehicles uncertainties, Journal of Energy Storage 25 (2019) 100812.

[21] Y. Cao, L. Huang, Y. Li, K. Jermsittiparsert, H. Ahmadi-Nezamabad, S. Nojavan, Optimal scheduling of electric vehicles aggregator under market price uncertainty using robust optimization technique, International Journal of Electrical Power Energy Systems 117 (2020) 105628.

[22] H. Ahmadi-Nezamabad, M. Zand, A. Alizadeh, M. Vosoogh, S. Nojavan, Multi-objective optimization based robust scheduling of electric vehicles aggregator, Sustainable Cities and Society 47 (2019) 101494.

[23] M. Ghahramani, S. Nojavan, K. Zare, B. Mohammadi-ivatloo, Short-term scheduling of future distribution network in high penetration of electric vehicles in deregulated energy market, in: Operation of distributed energy resources in smart distribution networks, Elsevier, 2018, pp. 139–159.

[24] M. N. Mojdehi, P. Ghosh, An on-demand compensation function for an EV as a reactive power service provider, IEEE Transactions on Vehicular Technology 65 (6) (2016) 4572–4583.

[25] H. Nafisi, S. M. M. Agah, H. A. Abyaneh, M. Abedi, Two-stage optimization method for energy loss minimization in microgrid based on smart power man-

agement scheme of PHEVs, IEEE Transactions on Smart Grid 7 (3) (2016) 1268–1276.

[26] V. K. Tumuluru, D. H. K. Tsang, A two-stage approach for network constrained unit commitment problem with demand response, IEEE Transactions on Smart Grid 9 (2) (2018) 1175–1183.

[27] M. A. Mirzaei, A. S. Yazdankhah], B. Mohammadi-Ivatloo, Stochastic security-constrained operation of wind and hydrogen energy storage systems integrated with price-based demand response, International Journal of Hydrogen Energy 44 (27) (2019) 14217–227.

[28] S. M. B. Sadati, J. Moshtagh, M. Shafie-khah, J. P. Catalão, Smart distribution system operational scheduling considering electric vehicle parking lot and demand response programs, Electric Power Systems Research 160 (2018) 404–418.

[29] Y. Xiong, B. Wang, C. cheng Chu, R. Gadh, Vehicle grid integration for demand response with mixture user model and decentralized optimization, Applied Energy 231 (2018) 481–493.

[30] H. Zhao, X. Yan, H. Ren, Quantifying flexibility of residential electric vehicle charging loads using non-intrusive load extracting algorithm in demand response, Sustainable Cities and Society 50 (2019) 101664.

[31] Z. Soltani, M. Ghaljehei, G. Gharehpetian, H. Aalami, Integration of smart grid technologies in stochastic multi-objective unit commitment: An economic emission analysis, International Journal of Electrical Power Energy Systems 100 (2018) 565–590.

[32] N. Hajibandeh, M. Shafie-khah, S. Talari, S. Dehghan, N. Amjady, S. J. P. S. Mariano, J. P. S. Cataláo, Demand response-based operation model in electricity markets with high wind power penetration, IEEE Transactions on Sustainable Energy 10 (2) (2019) 918–930.

[33] H. Wu, M. Shahidehpour, A. Alabdulwahab, A. Abusorrah, Thermal generation flexibility with ramping costs and hourly demand response in stochastic security-constrained scheduling of variable energy sources, IEEE Transactions on Power Systems 30 (6) (2015) 2955–2964.

[34] Y. Zhang, X. Han, M. Yang, B. Xu, Y. Zhao, H. Zhai, Adaptive robust unit commitment considering distributional uncertainty, International Journal of Electrical Power Energy Systems 104 (2019) 635–644.

[35] A. Velloso, A. Street, D. Pozo, J. M. Arroyo, N. G. Cobos, Two-stage robust unit commitment for co-optimized electricity markets: An adaptive data-driven approach for scenario-based uncertainty sets, IEEE Transactions on Sustainable Energy 11 (2) (2020) 958–969.

[36] N. Amjady, S. Dehghan, A. Attarha, A. J. Conejo, Adaptive robust network-constrained AC unit commitment, IEEE Transactions on Power Systems 32 (1) (2017) 672–683.

[37] J. Liu, C. Chen, Z. Liu, K. Jermsittiparsert, N. Ghadimi, An igdt-based risk-involved optimal bidding strategy for hydrogen storage-based intelligent parking lot of electric vehicles, Journal of Energy Storage 27 (2020) 101057.

[38] A. Ahmadi, A. E. Nezhad, B. Hredzak, Security-constrained unit commitment in presence of lithium-ion battery storage units using information-gap decision theory, IEEE Transactions on Industrial Informatics 15 (1) (2019) 148–157.

[39] A. Nikoobakht, J. Aghaei, IGDT-based robust optimal utilisation of wind power generation using coordinated flexibility resources, IET Renewable Power Generation 11 (2) (2017) 264–277.

[40] M. A. Mirzaei, A. Sadeghi-Yazdankhah, B. Mohammadi-Ivatloo, M. Marzband, M. Shafie-khah, J. P. Catalão, Integration of emerging resources in IGDT-based robust scheduling of combined power and natural gas systems considering flexible ramping products, Energy 189 (2019) 116195.

[41] A. Ahmadi, A. E. Nezhad, P. Siano, B. Hredzak, S. Saha, Information-gap decision theory for robust security-constrained unit commitment of joint renewable energy and gridable vehicles, IEEE Transactions on Industrial Informatics 16 (5) (2020) 3064–3075.

[42] A. Rabiee, A. Soroudi, A. Keane, Information gap decision theory based OPF with HVDC connected wind farms, IEEE Transactions on Power Systems 30 (6) (2015) 3396–3406.

[43] A. Soroudi, A. Rabiee, A. Keane, Information gap decision theory approach to deal with wind power uncertainty in unit commitment, Electric Power Systems Research 145 (2017) 137–148.

[44] S. Naghdalian, T. Amraee, S. Kamali, F. Capitanescu, Stochastic network-constrained unit commitment to determine flexible ramp reserve for handling wind power and demand uncertainties, IEEE Transactions on Industrial Informatics 16 (7) (2020) 4580–4591.

[45] N. Chakraborty, A. Mondal, S. Mondal, Efficient load control based demand side management schemes towards a smart energy grid system, Sustainable Cities and Society 59 (2020) 102175.

[46] X. Zhang, M. Shahidehpour, A. Alabdulwahab, A. Abusorrah, Hourly electricity demand response in the stochastic day-ahead scheduling of coordinated electricity and natural gas networks, IEEE Transactions on Power Systems 31 (1) (2015) 592–601.

[47] S. M. Moghaddas-Tafreshi, M. Jafari, S. Mohseni, S. Kelly, Optimal operation of an energy hub considering the uncertainty associated with the power consumption of plug-in hybrid electric vehicles using information gap decision theory, International Journal of Electrical Power Energy Systems 112 (2019) 92–108.

[48] A. Alabdulwahab, A. Abusorrah, X. Zhang, M. Shahidehpour, Stochastic

security-constrained scheduling of coordinated electricity and natural gas infrastructures, IEEE Systems Journal 11 (3) (2017) 1674–1683.

[49] M. A. Mirzaei, M. N. Heris, K. Zare, B. Mohammadi-Ivatloo, M. Marzband, S. Asadi, A. Anvari-Moghaddam, Evaluating the impact of multi-carrier energy storage systems in optimal operation of integrated electricity, gas and district heating networks, Applied Thermal Engineering (2020) 115413.

[50] M. Nazari-Heris, B. Mohammadi-Ivatloo, S. Asadi, Optimal operation of multi-carrier energy networks with gas, power, heating, and water energy sources considering different energy storage technologies, Journal of Energy Storage 31 (2020) 101574.

[51] M. A. Mirzaei, M. Nazari-Heris, B. Mohammadi-Ivatloo, K. Zare, M. Marzband, M. Shafie-Khah, A. Anvari-Moghaddam, J. P. Catalão, Network-constrained joint energy and flexible ramping reserve market clearing of power and heat-based energy systems: A two-stage hybrid igdt-stochastic framework, IEEE Systems Journal (2020) 1–10.